Available online at www.sciencedirect.com
SCIENCE DIRECT®
Journal of Nuclear Materials 351 (2006) 241–246
journal of nuclear materials
www.elsevier.com/locate/jnucmat

Nano-mesoscopic structural control in 9CrODS ferritic/martensitic steels

S. Ohtsuka *, S. Ukai, M. Fujiwara

Oarai Engineering Center, Japan Nuclear Cycle Development Institute, 4002 Narita-cho, Oarai-machi, Higashi-Ibaraki-Gun, Ibaraki-ken 311-1393, Japan

Abstract

Effects of varying oxygen concentration and final heat treatment on high-temperature strength and microstructure in 9Cr-oxide dispersion strengthened steel (9CrODS) were investigated. It was shown that appropriate control of excess oxygen concentration remarkably improves creep strength of 9CrODS. This creep strength improvement is ascribed to ultra-fine oxide particle dispersion in a part of the grains and increasing austenite (γ) to ferrite (α) diffusional transformation. Enhancement of austenite (γ) to ferrite (α) diffusional transformation leads to suppression of grain boundary sliding. Creep strength of 9CrODS can be remarkably improved by controlling excess oxygen concentration and performing a furnace-cooling heat treatment for austenite (γ) to ferrite (α) diffusional transformation.

PACS: 81.20.Ev; 62.20Hg; 28.50.Ft; 28.52.Fa

1. Introduction

9Cr-oxide dispersion strengthened martensitic steel (9CrODS) is viewed as an attractive candidate for advanced fast reactor (FR) fuel cladding because of its superior swelling resistance and improved creep strength. Japan Nuclear Cycle Development Institute (JNC) has been engaged in developing 9CrODS for FR cladding, and has successfully produced thin-walled tube with this material [1,2]. However, it was recently found that creep strength of 9CrODS cladding tube in hoop direction is inconsistent as shown in Fig. 1 [3], even though the same manufacturing process was applied to these tubes. The variability of creep strength is attributed to different amounts of oxygen contamination in the cladding tubes [3]. For the establishment of a consistently reliable manufacturing procedure, it is important to systematically clarify the effects of manufacturing conditions including oxygen concentration on mechanical properties of 9CrODS.

In this study, the effects of oxygen concentration and final heat treatment on the high-temperature strength and nano-mesoscopic structure in 9CrODS were investigated.

* Corresponding author. Tel.: +81 29 267 4141x5718; fax: +81 29 266 2904.
E-mail address: ohtsuka.satoshi@jaea.go.jp (S. Ohtsuka).

0022-3115/$ - see front matter © 2006 Elsevier B.V. All rights reserved.
doi:10.1016/j.jnucmat.2006.02.006

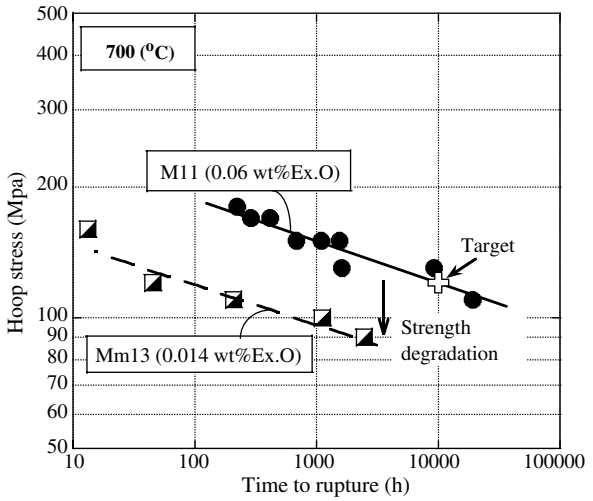

Fig. 1. Internally pressurized creep strength of 9CrODS steel cladding tubes [3].

2. Experimental procedures

9CrODS bars with 10 mm diameters were manufactured by mechanical alloying (MA) and hot-extrusion process. Element powder (iron (Fe), chromium (Cr), carbon (C), tungsten (W), titanium (Ti)), yttrium oxide (Y_2O_3) powder, iron–yttrium intermetallic compound (Fe_2Y) powder and iron oxide (Fe_2O_3) powder were mixed and mechanically alloyed in an attrition-type ball mill with a rotating speed of 220 revolutions per minute (rpm) for 48 h in Ar gas atmosphere. Oxygen concentration was controlled by adjusting the amount of Fe_2Y powder and Fe_2O_3 powder in the mixture. Y_2O_3 powder consists of approximately 20 nm diameter Y_2O_3 particles. The resulting mechanically alloyed powders (MA powders) were sealed in mild steel cans and degassed at 400 °C in 0.1 Pa vacuum. These powders were sintered by hot-extrusion at 1150 °C and air-cooled. The extruded bars were forged at 1150 °C and were either normalized (N: 1050 °C × 1 h, argon-gas cooling), normalized-and-tempered (NT: 1050 °C × 1 h, argon-gas cooling ⇒ 800 °C × 1 h, argon-gas cooling), or else furnace-cooled (FC: 1050 °C × 1 h ⇒ furnace-cooling at 30 °C/h). The cooling rate in normalizing-and-tempering heat treatment of the extruded bars is ~7000 °C/h, while that of the cladding tube is ~3000 °C/h as discussed in Section 3.3. The chemical compositions of the extruded bars were analyzed. The analyzed results are shown in Table 1, where Ex.O stands for excess oxygen which is defined as the value subtracting oxygen contents in Y_2O_3 powder from the total oxygen contents in steel. The extruded bar had a nominal composition of Fe–0.13wt%C, 9% Cr, 2% W, 0.2% Ti, and 0.35% Y_2O_3. Oxygen concentration was analyzed by inert gas fusion method [4]. The samples were fused in a graphite crucible under a flowing helium gas stream. The released oxygen combines with carbon from the crucible to form carbon monoxide. The carbon monoxide is oxidized to carbon dioxide by heated copper oxide and is carried by the flowing helium gas stream to an infrared detector to determine oxygen concentration.

Uni-axial tensile and creep tests were performed with a gage size of 6 mm diameter × 30 mm length at a temperature of 700 °C. The loading direction was parallel to the extrusion direction. The tensile tests were performed for normalized-and-tempered steels, while the creep tests were performed for both normalized-and-tempered steels and furnace-cooled

Table 1
Chemical composition of the 9CrODS

	Chemical composition (wt%)										
	C	Ni	Cr	W	Ti	Y	O	N	Ar	Y_2O_3[a]	Ex.O[b]
Y1	0.13	0.01	8.9	1.9	0.20	0.27	0.099	0.014	0.005	0.34	0.03
Y2	0.13	0.01	8.9	2.0	0.21	0.28	0.12	0.012	0.006	0.36	0.04
Y3	0.14	<0.01	8.9	2.0	0.21	0.28	0.18	0.010	0.005	0.36	0.10
E5	0.13	0.01	8.9	2.0	0.21	0.28	0.16	0.009	0.005	0.36	0.08
Mm15	0.14	0.01	9.0	2.0	0.20	0.28	0.17	0.006	0.004	0.36	0.09
M11 [3]	0.13	0.02	9.0	2.0	0.20	0.29	0.14	0.013	0.003	0.37	0.06
M12	0.13	–	9.0	1.9	0.21	0.28	0.15	–	0.005	0.36	0.07
Mm13 [3]	0.14	0.01	8.9	2.0	0.20	0.27	0.21	0.010	0.005	0.34	0.14
T3	0.13	0.01	8.8	2.0	0.21	0.27	0.22	0.012	0.005	0.34	0.15

[a] Estimated from yttrium concentration with assumption that yttrium exists as Y_2O_3.
[b] Estimated by subtracting the oxygen coupled with Y_2O_3 from the total amount of oxygen in steel.

steels. The loaded stress in the creep test was in the range from 80 to 180 MPa.

Metallographic examinations were performed using an optical microscope for both normalized steels and furnace-cooled steels. The etchant was a solution consisting of 50% aqua regia + 50% water. Diameter of prior austenite (γ)-grain was inferred from the optical microstructures.

For the purpose of examining austenite (γ) $\Rightarrow$ ferrite (α) transformation behavior of 9CrODS, continuous cooling transformation (CCT) diagram was drawn up by measuring diameter change during cooling at a constant rate of 50 $\sim$ 18 000 °C/h from 1150 °C $\times$ 1 h annealing.

3. Results and discussion

3.1. Mechanical properties

Dependence of uni-axial creep and tensile properties on excess oxygen concentration is shown in Fig. 2 [5]. Both creep strength and short-term strength are improved when excess oxygen concentration is around 0.08 wt%.

3.2. Microstructure

The representative optical microstructures of normalized steels and furnace-cooled steels are shown in Fig. 3. There is a clear difference of microstructure between the high creep strength steel (E5) and the low creep strength steel (T3, Y1). In normalized steels, both equiaxed and elongated grain co-exist in E5 (0.08 wt% excess oxygen), while only equiaxed grains are observed in T3 (0.15 wt% excess oxygen) and Y1 (0.03 wt% excess oxygen). As to the microstructures of furnace-cooled steels, grains in T3 and Y1 grow to a diameter of $\sim$10 μm, on the other hand, the grain size in E5 remains small. The prior austenite (γ) grain diameters are $\sim$3 μm for E5 and $\sim$10 μm for both T3 and Y1.

It was reported that severe plastic deformation in the MA process produces a powder matrix composed of ultra-fine ferrite (α) grains [6]. During the subsequent hot-extrusion process, both ferrite (α) to austenite (γ) phase transformation and grain growth simultaneously proceed. In high strength steel (E5), the hot-extrusion step seems to transform ultra-fine α-Fe grains to a dual phase microstructure consisting of austenite (γ) phase and retained ferrite (α) phase. If ferrite (α) phase completely transforms to austenite (γ) phase at hot-extrusion process, matrix grains totally become equiaxed, however, in E5, elongated grain remains as seen in Fig. 3. The elongated grain must be ferrite (α) grain, which remained without transforming to austenite (γ) phase during hot-extrusion process. In this study, we designate this elongated ferrite (α) phase as residual-α phase in order to distinguish the residual-α phase from ferrite (α) phase which is formed through austenite (γ) to ferrite (α) diffusional transformation in final heat treatment.

Previous transmission electron microscope (TEM) observations revealed that oxide particle diameter in elongated grain is much finer than in equiaxed grain and its diameter is $\sim$2 nm [5]. Higher oxide dispersion strengthening is expected in elongated grain than in equiaxed grain. It is supposed that the elongated residual-α phase remarkably enhances creep strength of 9CrODS.

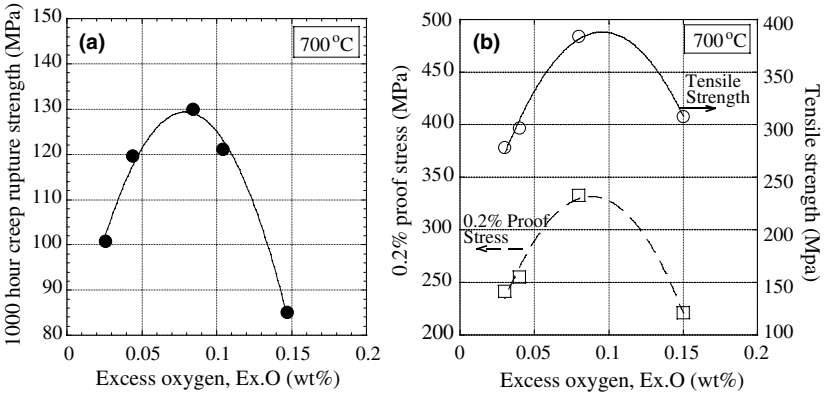

Fig. 2. Uni-axial creep and tensile property of 9CrODS bars containing different concentrations of excess oxygen [4], (a) 1000 h creep rupture strength, (b) 0.2% proof stress and tensile strength.

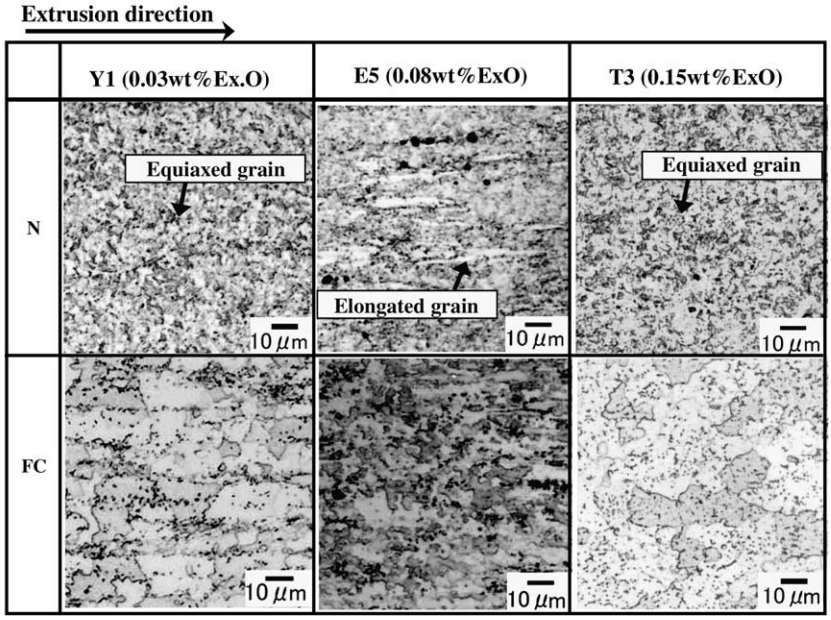

Fig. 3. Optical microstructures of 9CrODS steel bars after the normalizing (N) and the furnace-cooling (FC).

3.3. Continuous cooling transformation diagram

For examining the effects of cooling rate in final heat treatment on microstructure of 9CrODS, continuous cooling transformation (CCT) diagram was drawn using M12 bar (0.07 wt% Ex.O). M12 bar is assumed to have similar microstructure to E5 because it has approximately same concentration of excess oxygen. Austenite (γ) to ferrite (α) phase transformation is enhanced as size of prior austenite (γ)-grain decreases [7]. Grain boundary is a preferred nucleation site of carbide. Smaller prior austenite (γ)-grain provides a larger number of carbide precipitation. Nucleation of ferrite (α) from austenite (γ) phase should be enhanced at carbon-depleted area nearby carbide. Fig. 4 shows the CCT diagram, where the data of EM10 were also plotted for comparison. The EM10 was consolidated by a process consisting of cold isostatic pressing, 1100 °C × 1 h annealing and hot-extrusion of pre-alloyed EM10 powders atomized in argon gas [7]. The nominal composition of EM10 was Fe–0.088 wt%C, 8.5% Cr, 1.0% Mo, 0.50% Ni, 0.47% Mn, 0.37% Si [7]. The CCT diagram of M12 bar (solid circle) is quite different from that of EM10 (open diamond). Therefore maximal cooling rate (R_m) to produce a transformation of austenite (γ) to ferrite (α) in M12 is much higher than in EM10. This difference is attributed to the difference in prior austenite

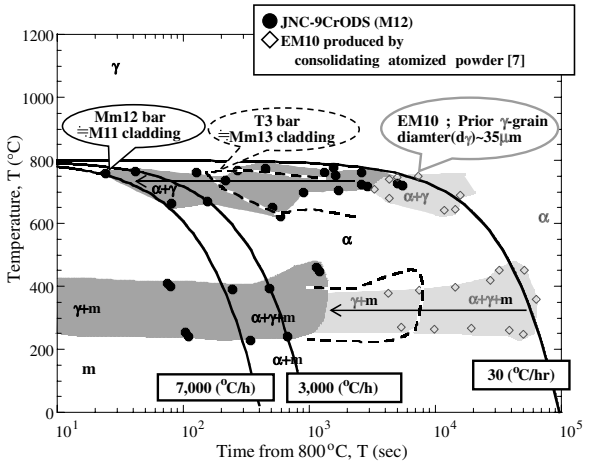

Fig. 4. Continuous cooling transformation (CCT) diagram of 9CrODS.

(γ)-grain size between M12 and EM10. The higher R_m in M12 than in EM10 is likely caused by smaller prior austenite (γ)-grain in M12 than in EM10. EM10 has large prior austenite (γ)-grain of 35 μm diameter [7], while M12 would have much smaller prior austenite (γ)-grain diameter of ~5 μm as inferred from optical micrograph in Fig. 3. M12 has ultra-fine oxide particle dispersion which suppresses grain growth by Zener pinning [8].

It is inferred from optical microstructures in Fig. 3 that prior austenite (γ)-grain size of T3 and

Y1 (~10 μm) is in between M12 and EM10. Therefore R_m of T3 and Y1 is in between M12 (8000 °C/h) and EM10 (100 °C/h) as shown with dotted line in Fig. 4. T3 and Y1 have the slower R_m than M12 and is easier to transform from austenite (γ) not to ferrite (α) but to martensite (α′) than M12.

In final heat treatment of cladding tubes, the cooling rate of the normalizing is ~3000 °C/h. Fig. 5 shows a temperature history of furnace atmosphere during the normalizing-and-tempering heat treatment. The atmosphere temperature is approximately the same as temperature of cladding tube, because the cladding tube has a thin wall of 0.5 mm thickness. Fig. 4 suggests that M11 cladding (0.06 wt% Ex.O), which is equivalent to M12 bar, should not completely transform from austenite (γ) phase to martensite (α′) phase and partially transform from austenite (γ) phase to ferrite (α) phase in the final heat treatment (~3000 °C/h). On the other hand, in Mm13 cladding (0.14 wt% Ex.O) which is equivalent to T3 bar, higher amount of austenite (γ) to _martensite (α′) phase transformation should take place than in M11 cladding because of the slower R_m in Mm13 than in M11. The increasing fraction of martensite phase cladding is expected to degrade creep strength of 9CrODS, because martensite phase has packet boundary which has random orientation and is easy to slide. As seen in Fig. 1, creep strength of 9CrODS cladding tube is inconsistent, although same manufacturing process was applied. One of the mechanisms of creep strength degradation in Mm13 compared to M11 would be the increasing fraction of martensite phase in Mm13.

The foregoing results imply that martensite phase (packet boundary) would degrade creep strength, while residual-α phase would remarkably enhance creep strength. Based on these insights, a procedure for further creep strength improvement was discussed in next section.

3.4. Effect of cooling rate on creep strength

Creep rupture tests of 9CrODS bars were performed after the normalizing-and-tempering and the furnace-cooling heat treatment. The test results are plotted on log–log scale in Fig. 6, together with the data of ferritic–martensitic steel (PNC-FMS) [9]. Here the normalizing-and-tempering was performed at a cooling rate of ~7000 °C/h, while furnace-cooling was performed at 30 °C/h. This means that most of austenite (γ) phase at 1050 °C annealing transforms to martensite (α′) phase during cooling process in the normalizing heat treatment. On the other hand, in the furnace-cooling treatment, the austenite (γ) phase totally transforms to ferrite (α) phase. Mm15 (0.09 wt% Ex.O) has elongated residual-α grain, while T3 (0.15 wt% Ex.O) does not have the elongated grain. It should be noticed that creep strength of Mm15 is superior to T3 after both the normalizing-and-tempering heat treatment and the furnace-cooling

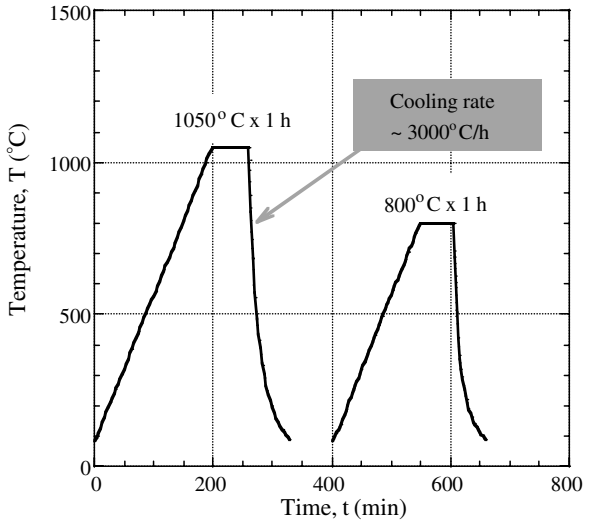

Fig. 5. Temperature history of furnace atmosphere in the normalizing-and-tempering (NT) heat treatment of 9CrODS cladding tube.

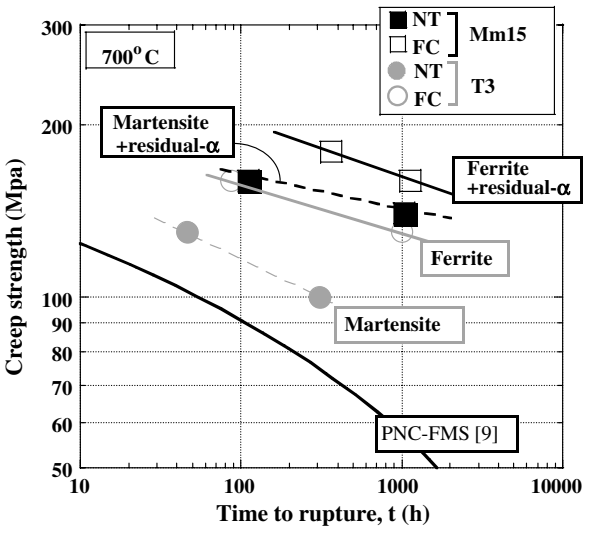

Fig. 6. Uni-axial creep strength of 9CrODS bars after the normalizing-and-tempering (NT) and the furnace-cooling (FC).

heat treatment. This is ascribed to the retention of the elongated residual-α phase in Mm15. Comparing the creep strength between normalized-and-tempered steel and furnace-cooled steel, the latter has apparently higher strength than the former. The microstructure of furnace-cooled steel does not contain martensite phase and packet boundary, while that of the normalized-and-tempered steels consists of fine martensite grain. This difference in microstructure would lead to lower grain boundary sliding in the furnace-cooled steels than in the normalizing-and-tempering steels. The dual phase composite microstructure consisting of ferrite (α) phase and residual-α phase would lead to an excellent creep strength improvement of 9CrODS.

4. Summary

In this study, investigation was performed on the effects of oxygen concentration and final heat treatment on the high-temperature strength and nano-mesoscopic structure in 9CrODS. Results can be summarized as follows:

(1) It was shown that appropriate control of excess oxygen concentration remarkably improves creep strength of 9CrODS. The creep strength improvement is apparently caused by retention of residual-α phase which has ultra-fine oxide particle dispersion.
(2) When excess oxygen concentration is around 0.08 wt%, prior austenite (γ) grain size remains small. This leads to enhancement of austenite (γ) to ferrite (α) diffusional transformation and decreasing fraction of martensite phase (packet boundary) in normalizing-and-tempering heat treatment. The decreasing fraction of martensite phase would contribute to suppression of grain boundary sliding and creep strength improvement.
(3) It was revealed that furnace-cooling heat treatment at a cooling rate of 30 °C/h leads to an excellent creep strength improvement of 9CrODS. This is ascribed to eliminating martensite phase by austenite (γ) to ferrite (α) diffusion transformation. It is supposed that composite structure consisting of ferrite (α) phase and residual-α phase leads to remarkable creep strength improvement.

Acknowledgement

The authors would like to express their great gratitude to associate professor Hideharu Nakashima (Kyushu University) for helpful discussions.

References

[1] S. Ukai, S. Mizuta, M. Fujiwara, T. Okuda, T. Kobayashi, J. Nucl. Sci. Technol. 39 (7) (2002) 778.
[2] S. Ukai, T. Nishida, H. Okada, T. Okuda, M. Fujiwara, K. Asabe, J. Nucl. Sci. Technol. 34 (3) (1997) 256.
[3] S. Ukai, T. Kaito, S. Ohtsuka, T. Narita, M. Fujiwara, T. Kobayashi, ISIJ Int. 43 (12) (2002) 2038.
[4] Standard JIS Z 2613-1992, General Rules for Determination of Oxygen in Metallic Materials.
[5] S. Ohtsuka, S. Ukai, M. Fujiwara, T. Kaito, T. Narita, J. Nucl. Mater. 329–333 (2004) 372.
[6] T. Okuda, M. Fujiwara, J. Mater. Sci. Lett. 14 (1995) 1600.
[7] V. Lambard, Development of ODS Ferritic–Martensitic Steels For Application to High Temperature and Irradiation Environment, RAPPORT CEA-R-5918, France, 2000.
[8] C. Zener quoted by C.S. Smith, Trans. Metall. Soc. AIME 75 (1948) 15.
[9] A. Uehira, S. Ukai, T. Mizuno, T. Asaga, E. Yoshida, J. Nucl. Sci. Technol. 37 (9) (2000) 780.